

Elsevier Editorial System(tm) for Applied Surface Science
Manuscript Draft

Manuscript Number:

Title: Integrated lithography to prepare periodic arrays of nano-objects

Article Type: Special Issue: APSUSC_E-MRS 2012 Symp V

Keywords: integrated interference and colloid sphere lithography; complex plasmonic structures; linearly and circularly polarized light

Corresponding Author: Dr. Mária Csete, PhD

Corresponding Author's Institution: University of Szeged

First Author: Mária Csete, PhD

Order of Authors: Mária Csete, PhD; Áron Sipos; Anikó Szalai

Manuscript Region of Origin: HUNGARY

Suggested Reviewers: Boris Luk'yanchuk Prof. Dr.
Data Storage Institute, Agency for Science, Technology and Research
Boris_L@dsi.a-star.edu.sg
expert in colloid sphere lithography

Dieter Bäuerle Prof. Dr.
Johannes Kepler University Linz Institute of Applied Physics
dieter.baeuerle@jku.at
expert in colloid sphere lithography

Paul Leiderer Prof. Dr.
Fachbereich Physik Universität Konstanz
paul.leiderer@uni-konstanz.de
expert in colloid sphere lithography



University of Szeged

Department of Optics and
Quantum Electronics

www.u-szeged.hu/optics/indexh.html

Dr. Mária Csete

H-6720 Szeged, Dóm tér 9.

✉ 6701 Szeged, Pf. 406

Phone.: (36-62) 544-528

Fax.: (36-62) 544-658

E-mail: mcsete@physx.u-szeged.hu

15 June 2012

Prof. H. Rudolph

Editor-in-Chief

Dept. of Physics & Astronomy,

Universiteit Utrecht,

Princetonplein 5, 3584 CC Utrecht,

Netherlands

Dear Professor Rudolph,

Enclosed please find our paper entitled “Integrated lithography to prepare periodic arrays of nano-objects” for special issue of **Applied Surface Science** devoted to *V symposium of EMRS conference*.

Yours sincerely:

Dr. Mária Csete

Integrated lithography to prepare periodic arrays of nano-objects

Áron Sipos, Anikó Szalai, Mária Csete

Department of Optics and Quantum Electronics, University of Szeged

H-6720 Szeged, Dóm tér 9, Hungary

HIGHLIGHTS

novel idea to integrate interference and colloid-sphere lithography

finite element method used to present the capabilities of integrated lithography

tuning four structure parameters independently by integrated lithography

illumination of silica sphere monolayer by two interfering beams

effect of wavelength, sphere diameter and polarization on near-field distribution



Strasbourg (France)

applied surface science

2012 – Symposium V

Laser materials processing for micro and nano applications

Paper number:

Manuscript Title: Integrated lithography to prepare periodic arrays of nano-objects

Corresponding Author: Dr. Mária Csete

Full Mailing Address: H-6720 Szeged, Dóm tér 9.,
☒ 6701 Szeged, Pf. 406

Telephone: (36-62) 544-528

Fax: (36-62) 544-658

E-mail: mcsete@physx.u-szeged.hu

Integrated lithography to prepare periodic arrays of nano-objects

Áron Sipos, Anikó Szalai, Mária Csete

Department of Optics and Quantum Electronics, University of Szeged

H-6720 Szeged, Dóm tér 9, Hungary

ABSTRACT

We present an integrated lithography method to prepare versatile nano-objects with variable shape and nano-scaled substructure, in wavelength-scaled periodic arrays with arbitrary symmetry. The idea is to illuminate colloid sphere monolayers by polarized beams possessing different lateral intensity distributions. Finite element method was applied to determine the effects of the wavelength, polarization and angle of incidence of the incoming beam, and to predict the shape of nano-objects, which can be fabricated on thin metal layer covered substrates due to the near-field enhancement under silica colloid spheres. The control of the inter-object distance is realized by varying the relative orientation of the periodic intensity distribution with respect to the silica colloid sphere monolayer. It is shown that illuminating silica colloid sphere monolayers by two interfering beams, linear patterns made of elliptical holes appear in case of linear polarization, while circularly polarized beams result in co-existent rounded objects, as circular nano-holes and nano-crescents. The size of the nano-objects and their substructure is determined by the spheres diameter and by the wavelength. We present various complex plasmonic patterns made of versatile nano-objects that can be uniquely fabricated applying the inherent symmetry breaking possibilities in the integrated lithography method.

Keywords: integrated interference and colloid sphere lithography, complex plasmonic structures, linearly and circularly polarized light

1. INTRODUCTION

Patterned surfaces consisting of objects having optional shape in the micro- and nanometric size range can be fabricated by classical methods of scanning beam lithography, like e-beam and ion-beam lithography [1]. These methods necessitate specific infrastructure, which is not widely available in science and industry. The rapidly developing nano-science and the closely related applications create a demand for relatively cheap fabrication methods, which are capable of reaching high resolution.

Interference lithography methods, which are generally based on the use of lasers, are comparatively cheap and effective methods to generate large-scale patterned surface areas, but require various complex techniques to overcome the diffraction limit [2]. Colloid particles have potential to change fundamentally the near-field distribution in their vicinity, and to overcome the diffraction limit [3]. The size of the colloid particle placed onto the surface and used to concentrate the light for machining has a dominant effect on the characteristics of the generated nano-features [4]. In addition to this, in colloid sphere lithography, one can tune the nano-feature parameters by using non-perpendicular incidence [5]. Although features with high versatility can be produced combining different approaches of colloid sphere lithography, these patterns all inherit the hexagonal symmetry of Hexagonally Close Packed (HCP) sphere monolayers [6]. Two main approaches are introduced in the literature to break the limits of the HCP symmetry: one is to control the assemblies construction by performing chemical modification of colloid spheres [7], while the second is to use pre-designed templates to determine the spheres' location [8]. Periodic illumination of sphere monolayers was

performed by applying different masks, but this method can result in only large-scale periodic changes in the surface structure [9].

In our present study we aim to present a special Integrated Interference and Colloid sphere Lithography (IICL) method, capable of resulting arrays having a period commensurate with the illuminating wavelength, where integration of the advantages of interference lithography and colloid-sphere lithography ensure a high degree of freedom in pattern generation of arbitrary rounded objects. Based on the potential to vary four structure parameters independently, this novel lithography method might revolutionize the fabrication of plasmonic [10] and meta-materials [11].

2. THEORETICAL METHODS

2.1 Integrated Interference and Colloid sphere Lithography realized by linearly and circularly polarized beams

In the proposed integrated lithography method hexagonal colloid sphere monolayers are illuminated by polarized beams possessing periodic lateral intensity modulation (Fig. 1). Theoretically, countable infinite number of sphere arrays might be selected by appropriate relative orientation and positioning of interference patterns with respect to hexagonal colloid sphere monolayers. The perfect synchronization of the intensity distribution and the sphere monolayer enables to confine the EM-field into nano-scaled areas under the colloid spheres shined at the intensity maxima, and to realize permanent substrate surface modification.

In our present study the periodic intensity distribution is defined by two interfering beams, as a result linear nano-object arrays might appear. Figure 1a shows the relative orientation of the plane of incidence ($\alpha=60^\circ$) and the periodic pattern ($\beta=30^\circ$) with respect to the (1, 0, 0) crystallographic direction selected for our present study, which is

denominated as IICL-II geometry in our previous works [12]. The $t_{II} = \sqrt{3} \cdot d$ inter-particle distance is predefined by the relative orientations specified by (α, β) angles. The period of the interference pattern can be tuned to $p_{II}^n = n \cdot d/2$ values by varying the λ wavelength and θ angle of incidence, based on the $p = \lambda/2 \cdot \sin \theta$ relationships between the periodicity and angle of incidence in case of two beam interference. The incidence angles corresponding to different n numbers might be computed as $\theta_{II}^n = \arcsin(\lambda/n \cdot d)$. In general case, the “ a ” and “ b ” axes of the holes are the characteristic nano-object size parameters, which might be tuned by the d diameter of the silica colloid spheres and by the λ wavelength, as in colloid sphere lithography. The near-field distribution might be influenced by illuminating analogous monolayers by linearly and circularly polarized beams with the same wavelength (Fig. 1).

2.2 Finite Element Method to determine the near-field distribution under silica colloid spheres

Finite Element Method was used to demonstrate the capabilities of IICL, by applying the COMSOL software package. The investigated model substrates are hexagonal monolayers of silica spheres with diameters of 100 nm, 250 nm and 500 nm, which are arrayed on 45 nm thin gold films covered NBK7 substrates. For all colloid sphere diameters beams with two different wavelengths (400 nm and 532 nm) were applied for illumination.

The applied numerical model is capable of studying off-axes illumination in conical mounting, in which the relative orientation of the plane of incidence with respect to $(1, 0, 0)$ crystallographic direction is specified by the α azimuthal angle (Fig. 1a), while the angle of incidence of the illuminating light beams is specified by the θ polar angle (Fig. 1b). Illumination of colloid sphere monolayers by perpendicularly incident

($\theta = 0^\circ$) homogeneous beams, which is referred as Homogeneous Illumination (HI), and by two interfering beams incident under analogous $\theta \neq 0^\circ$ angles were studied for both linearly and circularly polarized light (Fig. 2-4). The near-field enhancement under the colloid spheres is determined by dividing the maximal \mathbf{E} -field amplitudes at the colloid sphere – substrate interface by the amplitude of the incoming plane wave (Fig. 5a). The shape and size parameters of nano-objects, which might be fabricated by IICL, are determined based on the type and FWHM of the normalized \mathbf{E} -field distribution. The nano-holes are qualified by size parameters as the a and b axes of elliptical, and by the a diameter of circular holes. The $b-a/b$ flattening characterizing the degree of elongation of the nano-objects for cases of different illumination conditions are summarized in Fig. 5b. The flattening is 0 for a circular object, takes a positive value for horizontally and a negative for vertically elongated ellipses.

3. RESULTS AND DISCUSSION

When homogeneous beam is incident perpendicularly to the hexagonal monolayer of colloid spheres, hexagonal array of uniform holes might appear (Fig. 2-4/a, c, e, g). In case of linearly polarized light the holes are slightly elongated perpendicularly to the direction of \mathbf{E} -field oscillation, the degree of this elongation is larger under smaller spheres, and more pronounced, when 532 nm light illuminates the monolayer (Fig. 2-4/a-to-e). However the \mathbf{E} -field distribution observable under silica spheres significantly differs from the \mathbf{E} -field observed under metal spheres in our previous studies [12]. Perpendicularly incident circularly polarized homogeneous beam results in uniform intensity distribution under each colloid spheres, which is entirely rotationally symmetrical, i.e. arrays of uniform spherical holes may develop (Fig. 2-4/c, g).

Interestingly, in case of illumination by perpendicularly incident homogeneous 400 nm wavelength beam, the ratio of the nanoholes' predicted size to the diameter increases, when the sphere diameter decreases (Fig. 2-4/a, c). Similar tendency is not observable, when 532 nm wavelength, homogeneous beam illuminates the colloid sphere monolayer perpendicularly, on the contrary the predicted nanoholes' sizes decreases simultaneously with the diameter (Fig. 2-4/e, g).

Shining colloid sphere monolayers by two interfering polarized laser beams, i.e. with periodic intensity modulation corresponding to $n=6$ in CIICL-II geometry, linear patterns with analogous $3*d$ periodicity appears (Fig. 2-4/ b, d, f, h). These patterns are composed of elliptical nanoholes in case of linear polarization (Fig. 2-4/b, f), while co-existent almost circular nano-holes and nano-crescents can be prepared in case of circular polarization (Fig. 2-4/d, h). The nano-objects are less separated, when the sphere diameter decreases, independently from the polarization (Fig. 2->4/b, d, f, h). More separated nano-objects appear under the spheres with same diameter, when 532 nm wavelength beams are applied instead of 400 nm wavelength beams for all investigated colloid sphere monolayers (Fig. 2-4/ b-to-f, d-to-h).

3.1 Illumination of 500 nm diameter silica spheres in IICL-II geometry

The illumination of 500 nm diameter silica colloid spheres by perpendicularly incident homogeneous 400 nm and 532 nm wavelength beam results in hexagonal array of uniform nano-holes, with parameters slightly dependent on either of wavelength, or on polarization. Almost circular nano-holes appear with $a= 209$ nm and $b = 228$ nm axes in case of 400 nm wavelength beam (Fig. 2a), while elliptical holes are observable with $a = 209$ nm and $b = 316$ nm axes, when 532 nm linearly polarized light is applied for illumination (Fig. 2e). In case of circularly polarized light, circular holes can be

fabricated with diameters $a = 217$ nm at 400 nm, and $a = 239$ nm at 532 nm, i.e. only slightly dependent on the illumination wavelength (Fig. 2c, g).

When 500 nm diameter silica colloid sphere monolayers are illuminated in IICL-II geometry applying $\theta_{II}^{\circ} = 7.7^{\circ}$ incidence angle in case of 400 nm wavelength beam (Fig. 2b, d), and $\theta_{II}^{\circ} = 10.21^{\circ}$ in case of 532 nm wavelength beam (Fig. 2f, h), the interference maxima are aligned along colloid spheres at $t_{II} = 866$ nm distance, with $p_{II}^{\circ} = 1500$ nm periodicity according to the $n = 6$ case.

The complex pattern consists of central linear array of nano-holes, which are elongated horizontally with larger extent in case of 400 nm wavelength beams for both polarization, and with smaller extent in case of 532 nm wavelength linearly polarized beams, then the holes appearing as a result of HI at analogous wavelengths. Circularly polarized 532 nm wavelength beams result in circular holes, similarly to HI (Fig. 5a). The central hole array is surrounded by two neighboring linear array of similar spherical, and further two linear array of non-spherical, nano-crescent-like objects. Each of surrounding nano-objects is positioned at the spheres-substrate contact points, and surrounds the central nano-objects in a centrally symmetric hexagonal pattern. The central nano-objects are more circular, while the satellite nano-objects are more nano-petal-like, when circularly polarized light is applied instead of linearly polarized beams (Fig. 2/b,f-to-d,h) and when the illumination wavelength is modified from 400 nm to 532 nm (Fig. 2/b,d-to-f,h). As a result, the most versatile nano-objects might be prepared in case of illumination by 532 nm wavelength circularly polarized light.

3.2. Illumination of 250 nm diameter silica spheres in IICL-II geometry

When 250 nm diameter silica colloid spheres are illuminated by perpendicularly incident homogeneous beams, the size of the hexagonally arrayed uniform nano-holes

significantly decreases by changing the wavelength from 400 nm to 532 nm. In case of illumination by linearly polarized light not only the size, but the shape is also different at the two investigated wavelengths, similarly to 500 nm spheres. Namely, 400 nm wavelength beam results in circular nano-holes with $a = 134$ nm diameter (Fig. 3a), while application of 532 nm wavelength beam enables to fabricate elliptical holes with $a = 96$ nm and $b = 121$ nm axes (Fig. 3e). When circularly polarized light is applied for illumination, circular holes appear at both investigated wavelengths, having a diameter of $a = 134$ nm at 400 nm (Fig. 3c), and $a = 112$ nm at 532 nm (Fig. 3g), i.e. possessing more significantly wavelength dependent size parameters, than the holes appearing under 500 nm diameter silica spheres (Fig. 2-to-3/c, g).

In order to ensure the matching of $p_{II}^6 = 750$ nm periodic pattern with arrays composed by 250 nm diameter silica colloid spheres positioned at $t_{II} = 433$ nm distance corresponding to $n = 6$ case in IICL-II geometry, the hexagonal monolayer has to be illuminated by two interfering beams incident under $\theta_{II}^6 = 15.5^\circ$ angle in case of 400 nm wavelength (Fig. 3b, d), and under $\theta_{II}^6 = 20.8^\circ$ in case of 532 nm wavelength (Fig. 3f, h).

The complex pattern consists of a central linear array with two neighboring linear array of similar spherical nano-objects, and tiny satellite nano-objects appear under further two linear sphere arrays too. The surrounding nano-objects compose a centrally symmetric hexagonal pattern similarly to the pattern observed in case of 500 nm diameter spheres, but the satellites are shifted laterally from the spheres-substrate contact points towards the central nano-objects. In case of 400 nm wavelength, the nano-objects seem to be elongated along the **E**-field oscillation direction under 250 nm diameter silica spheres, more likely to the observation in case of metal spheres [12]. The

vertical elongation becomes less pronounced, when circularly polarized light is applied instead of linearly polarized beams (Fig. 3/b-to-d). Interestingly, the nano-object mini-arrays, that can be prepared in case of illumination by 532 nm wavelength linearly polarized light in IICL-II geometry, exhibits horizontal rather than vertical elongation, similarly to the nano-objects appearing in case of HI (Fig. 3f-to-e). In contrast, the arrays appearing due to circularly polarized 532 nm wavelength light illumination in IICL-II geometry exhibit vertical elongation similarly to the observation at 400 nm wavelength (Fig. 3d-to-h, Fig. 5a).

3.2 Illumination of 100 nm diameter silica spheres in IICL-II geometry

The intensity distribution as well as the shape and size of the hexagonally arrayed uniform nano-objects, that might be prepared by illuminating 100 nm diameter silica colloid spheres by perpendicularly incident homogeneous beams, significantly depends both on wavelength and polarization. Illumination by linearly polarized light results in nano-objects elongated perpendicularly to the **E**-field oscillation direction at both investigated wavelengths. The ratio of the axes ($a=53$ nm, $b=65$ nm) is smaller in case of 400 nm wavelength revealing slight elongation, while the largest ratio of axes lengths ($a=35$ nm, $b=66$ nm) indicates the highest degree of elongation at 532 nm wavelength (Fig. 4/a-to-e). Circularly polarized light illumination results circular holes' appearance at both investigated wavelengths, similarly to the 250 nm and 500 nm spheres, but the modification of the illumination wavelength results in the most pronounced decrease in diameters from $a = 57$ nm at 400 nm wavelength (Fig. 4c) to $a = 42$ nm at 532 nm wavelength (Fig. 4g).

Illumination of hexagonal monolayer in IICL-II geometry by two interfering beams incident under $\theta_{II}^{\circ} = 41.8^{\circ}$ angle in case of 400 nm wavelength (Fig. 4b, d), and under $\theta_{II}^{\circ} = 62.5^{\circ}$ in case of 532 nm wavelength (Fig. 4f, h) results in $p_{II}^{\circ} = 300 \text{ nm}$ periodic pattern matching linear arrays of 100 nm silica spheres positioned at $t_{II} = 173 \text{ nm}$ distance.

Less noticeable complex sub-structure appears as result that not only the central linear array, but also the neighboring linear sphere arrays are illuminated by interference maxima with finite extension. The resulted patterns consist of almost linear stripes with weak substructure in case of 400 nm wavelength revealing to vertically strongly elongated composing nano-objects (Fig. 4b, d). Centrally symmetric hexagonal pattern is recognizable only in complex structures appearing as a result of 532 nm light illumination (Fig. 4f, h). The nano-objects along the central array seem to be strongly elongated perpendicularly to the **E**-field oscillation direction in case of linear polarization due to the overlapping enhanced near-fields in the neighboring sphere arrays (Fig. 4f). In case of circular polarization slight vertical elongation is observable along the central array, and co-existent satellite nano-objects also appear, similarly to 250 nm spheres, only when 532 nm wavelength light is applied for illumination (Fig. 3,4/h). Mini-arrays of separated nano-objects can be prepared in IICL-II geometry only in case of illumination by 532 nm wavelength circularly polarized light of 100 nm diameter silica colloid spheres (Fig. 4h, Table I).

3.4. Quantitative near-field study

The **E**-field enhancement in IICL-II geometry is larger than in case of HI for both polarizations and for both wavelengths (Fig. 5a). This difference indicates that the intensity is more concentrated in IICL in comparison to HI. For 400 nm wavelength

light the enhancement decreases with the decrease of the diameter (Fig. 5a, blue bars), providing evidence about that the larger spheres are capable of better light concentration regardless of the polarization. For 532 nm wavelength light the enhancement is a non-monotonous function of the diameter (Fig. 5a, green bars). When the diameter changes from 500 nm to 250 nm, the enhancement decreases, while slightly higher concentration is observable, when e.g. 100 nm spheres are illuminated by homogeneous linearly polarized light, in accordance with the significant shape deformation observed on the near-field pictures (Fig. 4g).

The flattening characterizing the degree of nano-object elongation fundamentally depends on the illumination conditions (Fig. 5b). The homogeneous illumination with circularly polarized beams results in circular objects, i.e. the corresponding flattening is ~ 0 in all cases, i.e. bars with rectangular filling are missing from Fig. 5b. The illumination by homogeneous linearly polarized light shows similar tendencies for both wavelengths: the nano-objects are most circular under 250 nm diameter spheres, i.e. the flattening indicates minima at this diameter (Fig. 5b, bars with vertical lines). The flattening is larger for 532 nm wavelength beams in case of all investigated sphere diameters.

In IICL-II geometry, when 400 nm wavelength light is applied for illumination, the flattening switches from positive to negative values for both polarizations by decreasing the sphere diameter, indicating that vertically elongated nano-objects appear instead of horizontally elongated nano-holes (Fig. 5b, blue bars with tilted lines). For 532 nm, the tendency of flattening depends on the polarization, namely in case of linear polarization the nano-objects gradually gather horizontal elongation (Fig. 5b, green bars with tilted lines), while in case of circular polarization, the nano-objects become slightly vertically elongated, when the diameter decreases (Fig. 5b, green bars with crossed-tilted lines).

4. CONCLUSIONS

In our present work the capabilities of integrated interference and colloid sphere lithography are demonstrated for the case of illumination of silica colloid spheres by two interfering beams. By inspecting the near-field distribution under colloid spheres it is shown that four geometric parameters of nano-object arrays might be tuned in IICL. The relative orientation of the interference pattern and the monolayer determines the inter-object distance, the periodicity is defined by the angle of incidence, the nano-object shape and size is determined by the wavelength and sphere diameter, and is strongly influenced by the polarization of the light. The sensitivity of the nano-object orientation inside array to the experimental parameters will make possible to fabricate unique plasmonic and meta-materials with this novel integrated lithography.

ACKNOWLEDGEMENT

The study was funded by the National Development Agency of Hungary with financial support from the Research and Technology Innovation Funds (OTKA CNK-78549), and OTKA K 75149. The publication is supported by the European Union and co-funded by the European Social Fund. Project title: “Broadening the knowledge base and supporting the long term professional sustainability of the Research University Centre of Excellence at the University of Szeged by ensuring the rising generation of excellent scientists.” Project number: TÁMOP-4.2.2/B-10/1-2010-0012. The authors would like to thank Z. L. Horváth for the helpful discussions.

REFERENCES

- [1] B. D. Gates, Q. Xu, M. Stewart, D. Ryan, C. G. Wilson and G. M. Whitesides, New approaches to nanofabrication: molding, printing, and other techniques, *Chem. Rev.* 105 (2005) 1171-1196
- [2] C. Lu, and R. H. Lipson, Interference lithography: a powerful tool for fabricating periodic structures, *Laser & Photonic Reviews* 4(4) (2010) 568-580.
- [3] B. S. Luk'yanchuk, N. Arnold, S. M. Huang, Z. B. Wang, M.H. Hong, Three-dimensional effects in dry laser cleaning, *Appl. Phys. A* 77 (2003) 209-215.
- [4] B. S. Luk'yanchuk, Z B. Wang, W. D. Song, M. H. Hong, Particle on surface: 3D-effects in dry laser cleaning, *Appl. Phys. A* 79 (2004) 747-751.
- [5] W. Guo, Z. B. Wang, L. Li, D. J. Whitehead, B. S. Luk'yanchuk, and Z. Liu, Near-field laser parallel nanofabrication of arbitrary-shaped patterns, *Appl. Phys. Lett.* 90 (2007) 243101.
- [6] S.-M. Yang, S. G. Jang, D.-G. Choi, S. Kim, H. K. Yu, Nanomachining by Colloidal Litography, *Small* 2 (2006) 458-475
- [7] S. K. Smoukov, S. Gangwal, M. Marquez and O.D. Velev, Reconfigurable responsive structure assembled from magnetic Janus particles, *Soft. Matter* 5 (2009) 1285-92.
- [8] M. Rycenga, P. H. C. Camargo, Y. Xia, Template-assisted self-assembly: a versatile approach to complex micro- and nanostructures, *Soft Matter* 5 (2009) 1129-1136,.
- [9] J. H. Moon, W. S. Kim, J.-W. Ha, S. G. Jang, S.-M. Yang, J. K. Park, Colloidal lithography with crosslinkable particles: fabrication of hierarchical nanopore arrays, *Chem. Commun.* 32 (2005) 4107-4109..
- [10] J. B. Lassiter, H. Sobhani, J. A. Fan, J. Kundu, F. Capasso, P. Nordlander, N. J. Halas, Fano resonances in plasmonic nanoclusters: geometrical and chemical tunability, *Nano Letters* 10 (2010) 3184-3189.
- [11] V. Shalaev, Optical negative-index metamaterials, *Nature Photonics* 1 (2007) 41-48.
- [12] Á. Sipos, A. Szalai, M. Csete, Integrated lithography to prepare arrays of rounded nano-objects, in: William M. Tong (Ed.) *Proceeding of SPIE Vol. 8323*, SPIE, 2012 p 83232E

Figure 1. (a) The relative orientation of the plane of incidence (α), and the interference pattern (β), with respect to the (1, 0, 0) crystallographic direction in CIICL-II geometry. Inset indicates the a horizontal and b vertical axes of the elliptical nano-objects. (b) Illumination of hexagonal colloid sphere monolayers by two interfering linearly (straight arrow) and circularly (circular arrow) polarized beams is realized in CIICL-II geometry, where the θ_{ii}^n angle of incidence, the p_{ii}^n periodicity and the t_{ii} inter-object distance are also indicated.

Figure 2. Intensity distribution under 500 nm silica colloid spheres illuminated by 400 nm (upper row) and 532 nm (bottom row) linearly (first and second column) and circularly (third and fourth column) polarized light: (a, c, e, g) single perpendicularly incident beam, and (b, d, f, h) two beams interfering in IIICL-II geometry.

Figure 3. Intensity distribution under 250 nm silica colloid spheres illuminated by 400 nm (upper row) and 532 nm (bottom row) linearly (first and second column) and circularly (third and fourth column) polarized light: (a, c, e, g) single perpendicularly, incident beam, and (b, d, f, h) two beams interfering in IIICL-II geometry.

Figure 4. Intensity distribution under 100 nm silica colloid spheres illuminated by 400 nm (upper row) and 532 nm (bottom row) linearly (first and second column) and circularly (third and fourth column) polarized light: (a, c, e, g) single perpendicularly, incident beam, and (b, d, f, h) two beams interfering in IIICL-II geometry.

Figure 5. (a) Near-field enhancement under silica colloid spheres determined by dividing the maximal \mathbf{E} -field amplitudes at the colloid sphere – substrate interface by the amplitude of the incoming plane wave; (b) the $b-a/b$ flattening characterizing the degree of elongation determined for different conditions of HI and IICL-II geometry.

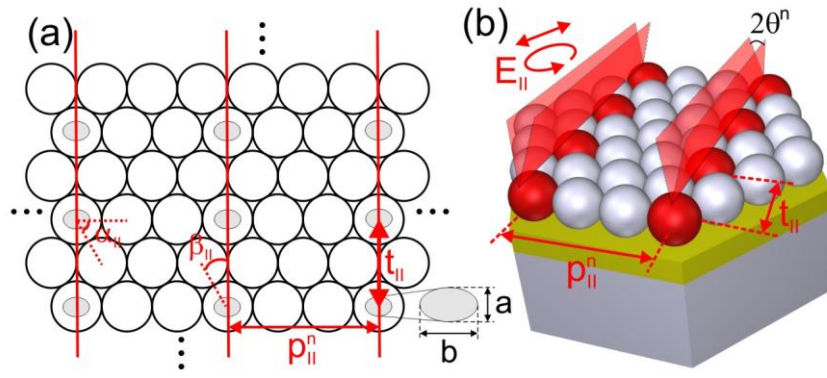


Figure 1

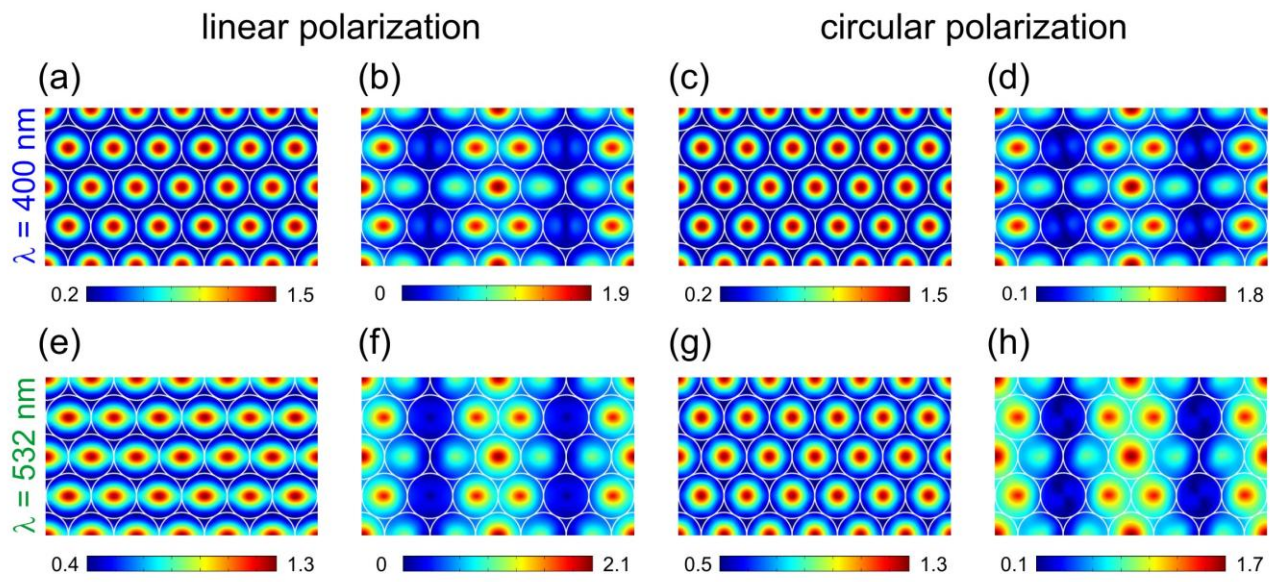


Figure 2

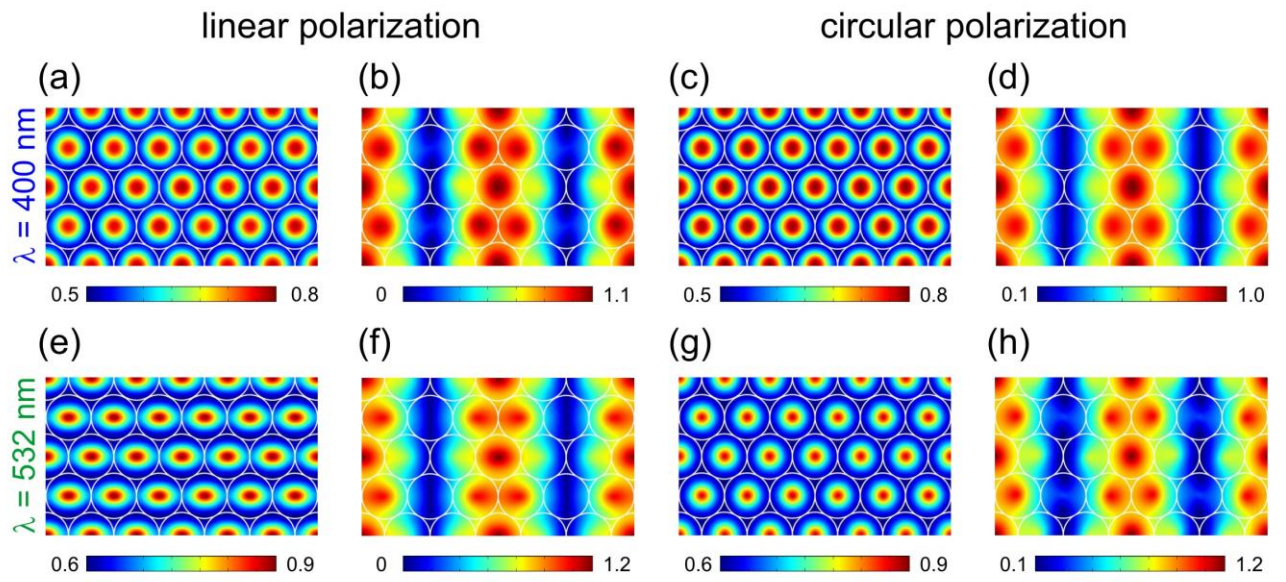


Figure 3

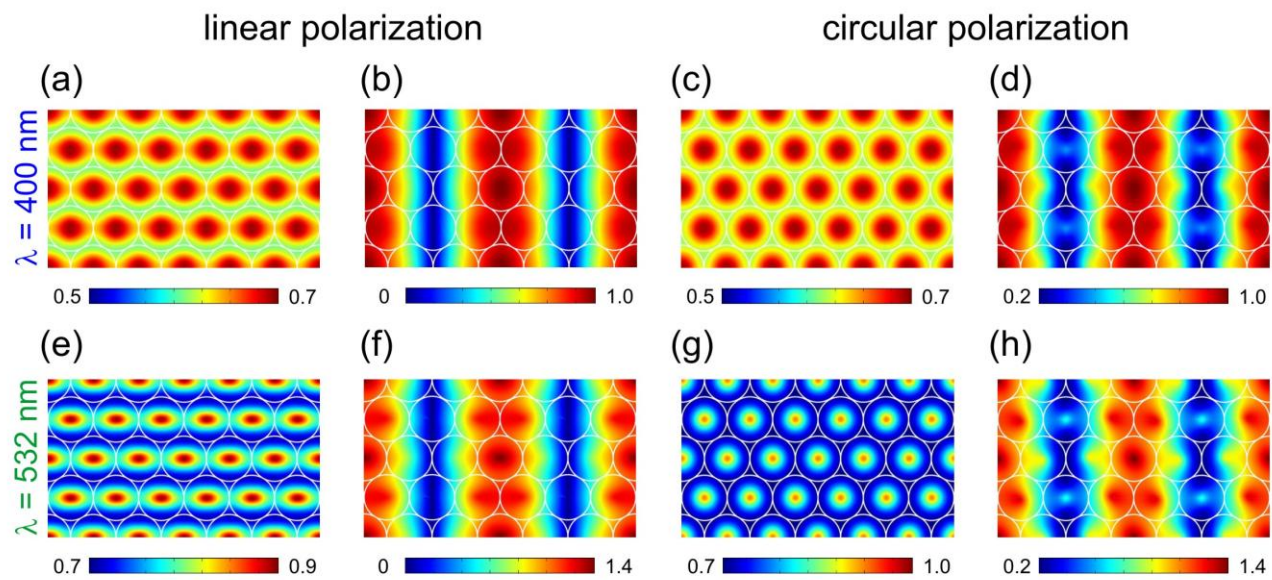


Figure 4

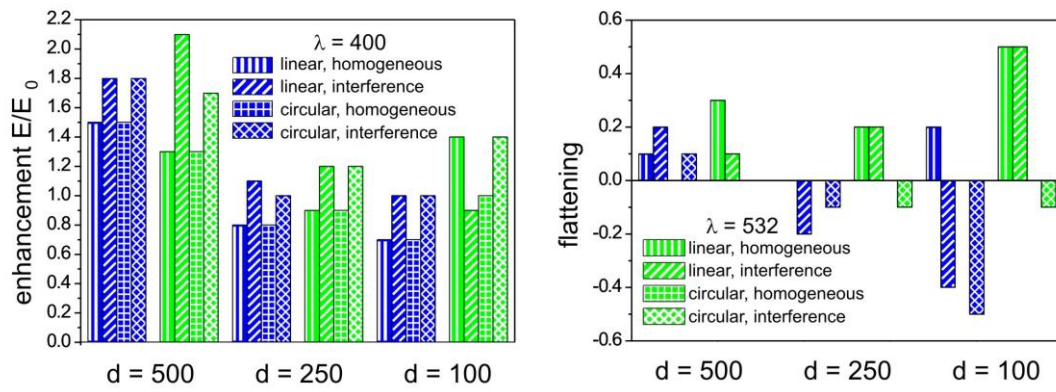


Figure 5